

Aberystwyth University

Quantifying Spatial and Temporal Vegetation Recovery Dynamics Following a Wildfire Event in a Mediterranean Landscape using EO Data and GIS

Petropoulos, George; Griffiths, Hywel; Kalivas, Dionyssos

Published in:
Applied Geography

DOI:
[10.1016/j.apgeog.2014.02.006](https://doi.org/10.1016/j.apgeog.2014.02.006)

Publication date:
2014

Citation for published version (APA):

Petropoulos, G., Griffiths, H., & Kalivas, D. (2014). Quantifying Spatial and Temporal Vegetation Recovery Dynamics Following a Wildfire Event in a Mediterranean Landscape using EO Data and GIS. *Applied Geography*, 50, 120-131. <https://doi.org/10.1016/j.apgeog.2014.02.006>

General rights

Copyright and moral rights for the publications made accessible in the Aberystwyth Research Portal (the Institutional Repository) are retained by the authors and/or other copyright owners and it is a condition of accessing publications that users recognise and abide by the legal requirements associated with these rights.

- Users may download and print one copy of any publication from the Aberystwyth Research Portal for the purpose of private study or research.
- You may not further distribute the material or use it for any profit-making activity or commercial gain
- You may freely distribute the URL identifying the publication in the Aberystwyth Research Portal

Take down policy

If you believe that this document breaches copyright please contact us providing details, and we will remove access to the work immediately and investigate your claim.

tel: +44 1970 62 2400
email: is@aber.ac.uk

Manuscript Number: JAPG-D-13-00306R3

Title: Quantifying Spatial and Temporal Ecosystem Recovery Dynamics following a wildfire event in a Mediterranean landscape using EO data and GIS Techniques

Article Type: Article

Keywords: Keywords: vegetation regeneration, fires, Landsat TM, ASTER DEM, NDVI, Greece

Corresponding Author: Dr. George Petropoulos,

Corresponding Author's Institution:

First Author: George Petropoulos

Order of Authors: George Petropoulos; Hywel M Griffiths; Dionissios P Kalivas

Abstract: Analysis of Earth Observation (EO) data, often combined with Geographical Information Systems (GIS), allows monitoring of changing land cover dynamics which may occur after a natural hazard such as a wildfire. In the present study, the vegetation recovery dynamics of one such area are evaluated by exploiting freely distributed EO data and GIS techniques. The relationships of re-growth dynamics to the exposure under topographical characteristics of the burn scar are also explored. As a case study, a typical Mediterranean ecosystem in which a wildfire occurred during 2007 is used. Vegetation recovery dynamics of the whole area under the burn scar were investigated based on chronosequence analysis of the normalized difference vegetation index (NDVI) derived from anniversary Landsat TM images. The spatio-temporal patterns of post-fire NDVI on each image date were statistically compared to the pre-fire pattern to determine the extent to which the pre-fire spatial pattern was re-established and the recovery rate. The relationships between NDVI as an expression of recovery rates and aspect were also statistically investigated and quantified using a series of statistical metrics. Results suggested a generally low to moderate vegetation recovery of the local ecosystem five years after the fire event, with the post-fire NDVI spatial pattern generally showing a gradual but systematic return to pre-fire conditions. Re-growth rates appeared to be somewhat higher in north-facing slopes in comparison to south facing ones, in common with other similar studies in Mediterranean type ecosystems. All in all, this study provides an important contribution to the understanding of Mediterranean landscape dynamics, and corroborates the usefulness particularly of NDVI in post-fire regeneration assessment via a well-established methodology presented herein which can also be transferable to other regions. It also provides further evidence that use of EO technology which combined with GIS techniques can offer an effective practical tool for mapping wildfire vegetation dynamics and ecosystem recovery after wildfire.

39 **1. INTRODUCTION**

40 Altering land cover dynamics is currently regarded as the single most important
41 variable of global change affecting ecological systems (Otukei and Blaschke, 2010).
42 Wildfires are considered to be one of the most widespread ecological disturbances of
43 natural ecosystems that dramatically affect land cover dynamics at a variety of spatial and
44 temporal scales as a result of the complete or partial removal of vegetation cover
45 (Lhermitte et al., 2011). In this context, knowledge of the spatio-temporal distribution of
46 post-fire vegetation recovery dynamics is of key importance. Such information plays a
47 significant role in various aspects of policy and decision-making as well as in the dynamics
48 and structures of plant and animal communities of the affected ecosystems (Elvira and
49 Hernando, 1989; Gouveia et al., 2010). Knowledge of vegetation recovery dynamics
50 following a fire outbreak is essential to estimate the effects of the fire and to understand the
51 forces driving changes in post-fire ecosystems (Grissino-Mayer and Swetnam, 2000; Casady
52 and Leeuwen, 2009). Such information, if available in a consistent, repetitive and cost-
53 effective manner, is also a crucial element of successful landscape management (Wittenberg
54 et al., 2007). It can assist in identifying areas needing intensive or special restoration
55 programs aiming to reduce soil erosion and runoff, thus mitigating long-term site
56 degradation (Keeley, 2000; Malak and Pausas, 2006; Gouveia et al., 2010). Given that future
57 changes in climate could potentially lead to increases in fire frequency, severity and extend
58 into ecosystems that include species that have not evolved to be able to easily regenerate
59 (Politi et al., 2009), information on regeneration vegetation is of key importance.

60 The speed of vegetation recovery can control the extent of various environmental,
61 social, economic and political impacts (Minchella et al., 2009). Indeed, the rate of vegetation
62 biomass re-growth can vary significantly; some areas can show complete vegetation
63 recovery after a few years while others are still not completely recovered decades after the
64 fire. In the Mediterranean region in particular where fire has been an important ecological
65 factor for millennia (Naveh, 1974; Mayor et al., 2007), rates of post-fire recovery dynamics
66 are usually spatially variable and contingent upon a number of factors. This is because of
67 the complexity of landscape structure and the range of responses of such systems to the
68 diverse types of fire regimes. At the landscape level, various studies have shown post-fire
69 regeneration to be mainly dependent on the initial vegetation and site-specific climatic and
70 terrain parameters (Pausas and Vallejo, 1999; Wittenberg et al., 2007). Climatic factors,
71 such as heavy autumn rainfalls, generally also lead to a higher potential for post-fire soil
72 erosion (Millán et al., 1995), which also affect vegetation re-growth dynamics (Pausas et al.,
73 2004). Moreover, various studies have shown that in such environments, post-fire growth is
74 frequently affected by topography and aspect. South-facing slopes experience higher
75 insolation and evapotranspiration rates than north-facing slopes. This results in vegetation
76 tending to grow back more quickly on north-facing slopes with more favourable moisture
77 conditions (Mouillot et al., 2005; Fox et al., 2008). Unfortunately, interactions between such
78 parameters and plant regeneration are poorly known, especially at the scale of a single
79 large fire. At this scale, use of Earth Observation (EO) technology has proved to be a suitable
80 option tool for monitoring plant regeneration after fire.

81 When combined with Geographic Information Systems (GIS) techniques, EO data
82 have demonstrated promising potential in providing an effective set of tools for analysing
83 and extracting spatial information related to wildfires (Chen et al., 2005; Durduran, 2010;
84 Chen et al., 2011; Kalivas et al., 2013). This integration provides an excellent framework for

85 data capture, storage, synthesis and analysis of acquired spatial data. Indeed, EO data can be
86 combined with GIS and can provide an efficient approach for analysing and extracting
87 spatial information to support decision making reliably and consistently (Chen et al., 2005;
88 Gens, 2010). Both have been used extensively in a range of post-fire applications at different
89 scales of observation; from burnt area mapping (Kokaly et al., 2007; Petropoulos et al.,
90 2011), to mapping changes in soil erosion after fire (Quintano et al., 2006; Mayor et al.,
91 2007; Fox et al., 2008) to evaluating post-fire ecosystem recovery (Segah et al., 2010). The
92 recent advancements in EO technology have made it possible to evaluate patterns of
93 vegetation recovery after wildfires at different spatial, spectral and temporal scales, and a
94 variety of techniques have been developed for this purpose.

95 Some of the most widely used image analysis approaches employed to characterize
96 the vegetation recovery include image classification (Jakubauskas et al., 1990; White et al.,
97 1996; Viedma et al., 1997; Hall et al., 1991; Steyaert et al., 1997; Stueve et al., 2009), the use
98 of spectral vegetation indices (Diaz-Delgado et al., 2003; Hope et al., 2007; Lhermitte et al.,
99 2011; Chen et al., 2011) and Spectral Mixture Analysis (Smith et al., 2007; Solans Vila and
100 Barbosa, 2010; Veraverbeke et al., 2012). Out of the wide range of techniques available,
101 spectral indices have been used evidently most extensively (Veraverbeke et al., 2010). Their
102 use has largely been based on the hypothesis that the ratio of red (R) to near infrared (NIR)
103 reflectance for green vegetation changes when the foliage containing chlorophyll is
104 destroyed by the fire. Subsequently, the use of a spectral index that is sensitive to the R and
105 NIR regions of the electromagnetic spectrum can be used to identify and potentially
106 quantify vegetation change. The most widely used index for studying regeneration
107 processes is the Normalized Difference Vegetation Index (NDVI, Rouse et al., 1973). NDVI
108 combines the reflectance in the R and NIR spectral region and is a measure of the green
109 vegetation amount. A significant number of studies have utilized this index to monitor post-
110 fire vegetation dynamics, some conducted in Mediterranean climates (Roder et al., 2008;
111 Solans Vila and Barbosa, 2010; Veraverbeke et al., 2010). Also, although a wide range of EO
112 data have been exploited in such studies, it is evident from a review of the literature that
113 imagery from the Landsat series of platforms has been one of the most widely exploited.

114 Landsat is the only freely-available multispectral satellite high spatial resolution
115 sensor providing a synoptic coverage of the Earth extending back to 1972. Therefore, the
116 value of data from this satellite radiometer is unique and they have been extensively used to
117 monitor the spatial and temporal variations in post-fire vegetation conditions and
118 landscape-scale trends in vegetation dynamics (Hope et al., 2007; Wittenberg et al., 2007;
119 Chen et al., 2011). Landsat spatial resolution allows the detection of both large and small
120 fires and its large sensor field of view allows the observation of several burnt areas in one
121 image. The sensor also has a NIR band which is useful for evaluating vegetation recovery
122 processes (Pereira et al., 1999). Furthermore, its shortwave infrared (SWIR) channels allow
123 highlighting of the internal variability of burnt areas that can be linked to the spatial
124 patterns of damage severity and fire intensity (Justice et al., 1993; Bisson et al., 2008).

125 Yet, while remote sensing is currently being applied to estimate the vegetation
126 recovery dynamics in different ecosystems, information on the relationships between post-
127 fire recovery and topographic factors is scarce (e.g. Sunee et al., 2001), particularly so in the
128 Mediterranean. This is despite the importance of this issue, as for example identification, at
129 the landscape level, of areas with low recovery dynamics could improve land management
130 and help prioritizing post-fire restoration actions in the fire-affected areas. Results from
131 relevant studies published so far suggest that vegetation recovery dynamics of south-facing

132 slopes can be very different from that of north-facing ones (e.g. Hope et al., 2007;
133 Wittenberg et al., 2007; Fox et al., 2008).

134 In this context, the main aim of this study has been to assess vegetation recovery
135 dynamics following a fire event using multi-temporal analysis of Landsat Thematic Mapper
136 (TM) images and GIS techniques for a typical Mediterranean characteristics site located in
137 Greece for which a wildfire occurred in 2007. The specific objectives were: first to determine
138 the spatio-temporal patterns of vegetation re-growth dynamics established within the burn
139 scar monitored by the NDVI response and second to analyse the influence of topographical
140 parameters on these dynamics. In this preliminary study, we attempted to fit regression
141 models to the dynamics of the regeneration process and to quantitatively investigate the
142 correlation between post-fire recovery and topographic factors (slope and aspect) using EO
143 data.

144

145 **2. STUDY AREA**

146 The selected study site, Mt. Parnitha, is located approximately 30 km north of the
147 Greek capital Athens (Figure 1). The area covers approximately 200 km² of land with an
148 altitude ranging from 200-1,400 m above sea level (a.s.l.). The region is covered mainly by
149 Greek Fir (*Abies cephalonica*) and Aleppo Pine (*Pinus halepensis*) forests on the slopes
150 beneath 1,000 m altitude, grasses and shrubs dominate above 1,000m, and under 300m
151 farmlands dominate to the north with suburban housing to the east. The climate is
152 continental, characterised by cold winters and warmer summers. Summer temperatures do
153 not usually exceed 18°C, while in winter temperatures are frequently of around 0°C,
154 (Arianoutsou et al., 2010), with an annual average of 11°C (Ganatsas et al., 2012). Average
155 rainfall in the area is 822 mm (at 1,000 m elevation), with 70 rainy days per year. Snow is
156 also relatively common, with an average of 33 snowy days per year and snow depth
157 averaging 120 cm (Ganatsas et al., 2012).

158 In the summer of 2007, Greece was hit by the most devastating large fires in its
159 recent history (Kalivas et al., 2013). During the first half of that year average monthly
160 temperatures in the study area increased from 11°C in January 2007 to 26°C in June (NOAA
161 web site, 2013). The maximum monthly temperature in June reached 39°C and there were
162 12 days in which the temperature rose above 32°C. On June 27th, 2007, at 19:30 local time, a
163 fire, caused by sparks from an overloaded power line, erupted in the area of Dervenohoria,
164 near a village called Stefani, approximately 15 km west of the core of mount Parnitha
165 National Park. On the next day, fanned by a medium strength west wind, it entered the
166 forested western slopes and canyons of the mountain and spread to the summit leaving
167 only charred trees. Its main run stopped when it reached sparse vegetation on the east
168 slope of the mountain in the morning of June 29th. Fought by aerial fire-fighting support, it
169 was controlled three days later (July 1st, 2007). According to official estimates, the total area
170 burnt was in the order of 45 Km² (Petropoulos et al., 2010).

171 Mt. Parnitha is a very suitable study site for this type of research from both scientific
172 and practical aspects. First of all, it is one of the few mountains surrounding Athens, the
173 capital of Greece, playing a very important role in the micro-climatic conditions of the
174 capital. Second, due to its rich biodiversity the wider area has been designated as a national
175 park as well as a biodiversity conservation site. It has also been included in the European
176 network of protected areas Natura 2000 EC Habitats Directive, a network of Sites of

177 Community Importance and Special Areas of Conservation (Arianoutsou et al., 2010). Thus
178 the area has a very significant ecological and aesthetic/recreational value for the local
179 people. Third, the region is characterized by very variable topography characteristics,
180 comprising plain areas and mountainous areas with slopes varying from between 3 % and
181 90 %, which vary significantly in elevation and aspect. In particular, altitude varies from
182 200 m.a.s.l to over 1,400 m.a.s.l (the highest elevation being 1,413 m.a.s.l.). Soils in the area
183 are generally shallow and infertile, with the exception of some karstic plateaus, and overly
184 bedrock consisting of sedimentary schists and limestone (Ganatsas et al., 2012). Fourth, all
185 data required were already available from previous works conducted in the region
186 (Petropoulos et al., 2010; 2011; 2012), and as such, the present work also builds on these
187 previous studies conducted in the area.

188

189 **3. DATASETS**

190 Five Landsat TM images (path: 183, row: 33 / raster format) were used in this study
191 to explore the vegetation regeneration dynamics of the selected study region over a period
192 of 5 years, from 2007 to 2011. Images around the same dates ('anniversary dates'; Lillesand
193 and Kiefer, 2000) of different years were selected to circumvent the influence of seasonal
194 differences in both spectral radiation (e.g. Sun elevation angle, Sun-Earth distance,
195 meteorological conditions) and surface reflection. A TM pre-fire image acquired on 16 May
196 2007 and four post-fire images acquired on 3 July 2007, 24 July 2009, 12 August 2010 and
197 15 August 2011 were used. All images were obtained from the United States Geological
198 Survey (USGS) archive (<http://glovis.usgs.gov/>) at no cost. They were acquired
199 geometrically corrected, geometrically resampled, and registered to a geographic map
200 projection with elevation correction applied (Level-1T processing).

201 In addition, the Global Digital Elevation Model (GDEM) of the Advanced Spaceborne
202 Thermal Emission and Reflection Radiometer (ASTER) sensor was used for obtaining
203 topographical information about the study area. The ASTER GDEM product was released in
204 2009 and was updated (Version 2) at the end of 2011. Estimated accuracies of the product
205 are for 20 meters at 95 % confidence for vertical data and 30 meters at 95 % confidence for
206 horizontal data (ASTER GDEM, 2009). The dataset is provided in geotiff format, in
207 geographic lat/long projection and WGS84/EGM96 datum. It is available to download at no
208 cost from the Earth Remote Sensing Data Analysis Center (ERSDAC) of Japan or the NASA's
209 REVERB (<http://reverb.echo.nasa.gov/>). ASTER GDEM is distributed as separate tiles of
210 elevation data. Herein, the tile covering the study site was acquired from REVERB.

211 Last but not least, an estimate of the burnt area was obtained from work that had
212 been carried out previously in the study area. In particular, Petropoulos et al., (2011)
213 obtained a burnt area cartography from the analysis of the same TM post-fire imagery used
214 herein, acquired shortly after the fire extinction (i.e. July 3rd, 2007) by applying a pixel-
215 based classifier based on Support Vector Machines (Vapnik, 1995).

216

217 **4. METHODS**

218 All analysis of the vegetation regeneration for the studied region was carried out
219 using ENVI (v. 5.0, ITT Visual Solutions) and ArcGIS (v. 10.1, ESRI) software platforms. An
220 overview of the methodology implemented is depicted in Figure 2.

221

4.1 Data Pre-processing

All pre-processing of the spatial datasets were carried out in ENVI. TM images pre-processing entailed a series of steps (Figure 2). First, for each date of TM image acquired, each spectral band was imported to ENVI and was converted to top of the atmosphere reflectance (TOA) according to the methodology described by Irons (2011). Subsequently, all the spectral bands from each acquisition date excluding the thermal infrared (i.e. band 6) were layer stacked to form a single image file corresponding to the acquisition date. Then, an empirical line normalization to all images was implemented using the pre-fire Landsat image (acquisition date: May 16th 2007) as a base (ENVI User's Guide, 2008). This is a relative atmospheric correction method which provides an easy way to correct for radiance/reflectance variations due to solar illumination condition, phenology and detector performance degradation (Latifovic et al., 2005). No further topographic correction was necessary as images were already terrain corrected. Next, the slope and aspect maps of the study region were computed from the ASTER GDEM (i.e. elevation map). Subsequently, image to image co-registration between the TM images and the ASTER DEM was performed.

In order to analyze imagery from different dates, the data layers must be spatially co-registered so that satellite data are in the same spatial reference frame (Schmidt and Glasser, 1998). The TM pre-fire image was used as a base image to which all other available images were co-registered. Approximately 45 commonly identified ground control points (GCPs) were selected randomly from easily detectable corner points (e.g. road junctions). Image warping was performed by applying the nearest neighbour method, allowing a co-registration of all the images into a common UTM 34N projection under a WGS84 ellipsoid. This resampling method was used to better preserve the digital number (DN)/reflectance values in the original images. To check the co-registration accuracy, the coordinates of 15 additional control points not previously included in the transformation were determined from the base image used. Displacement of these points relative to the other images was examined and results showed a positional accuracy within the sensor pixel range (i.e. < 30 m), which was considered satisfactory.

Then, the TM images and the ASTER DEM were layered stacked and subsequently clipped to a smaller area covering an area that included the burn scar and sufficient ample land outside its perimeter. This allowed us to enhance the computational efficiency of the processing that would follow. Next, this dataset was intersected with the burnt area polygon. This last dataset was the one used in analysing the vegetation dynamics occurring within the burn scar area of the Mt. Parnitha region. Some of the datasets derived after the end of pre-processing are illustrated in Figure 3.

4.2 Vegetation re-growth mapping

The approach used to detect the vegetation recovery rate for the fire-affected area for the whole area under the burn scar is shown in Figure 2. Vegetation dynamics of re-growth after the fire was evaluated through multi-temporal analysis of the NDVI. The latter was calculated from the R and NIR bands of each pre-processed TM image using the formula originally proposed by Rouse et al., (1973):

$$NDVI = \frac{\rho_{NIR} - \rho_R}{\rho_{NIR} + \rho_R} \quad (1)$$

265 where ρ_{NIR} and ρ_{R} denote the near-infrared and the red surface spectral
266 reflectance respectively. NDVI values can in theory scale between -1 and +1. The
267 photosynthetic activity in plants, and their ability to strongly reflect NIR radiation, is
268 expressed by lower reflectance in R and higher reflectance in NIR. As values approach +1,
269 photosynthetic activity becomes very strong. Thus, NDVI is an expression related to the
270 amount of photosynthetically active vegetation exposed to the sensor within each pixel, and
271 typical NDVI values for vegetated areas are in general well above 0.1 (Jensen, 2000;
272 Petropoulos and Kalaitzidis, 2011). Designed to capture the contrast between R and NIR
273 reflection of solar radiation by vegetation, NDVI has been widely used in studies of
274 vegetation phenology dynamics and inter-annual variability of vegetation greenness with
275 different types of EO data including Landsat (Gouveia et al., 2008) and has proved to be
276 particularly useful for monitoring post-fire plant regeneration dynamics (Gouveia et al.,
277 2010).

278 Following the NDVI computation for each TM image, the derived NDVI layers were
279 layered stacked to the pre-processed dataset (section 4.1) to form a single dataset to
280 facilitate further analysis in the GIS environment. The dynamics of the regeneration process
281 were subsequently analysed by comparing post-fire NDVI spatial patterns to the pre-fire
282 pattern. This allowed determining the extent to which the pre-fire pattern was re-
283 established, and the rate of this recovery. In accordance to previous works (e.g. Hope et al.
284 2007), descriptive statistics of NDVI within the burn scar were computed from each TM
285 image, which together with scatter plot and non-parametric correlation analysis were used
286 in evaluating the NDVI variations under the burnt area envelope.

287 In the next step, relationships between vegetation recovery dynamics and aspect
288 were investigated. Aspect analysis was conducted in ArcGIS using the aspect map produced
289 from the ASTER GDEM. In accordance to previous studies (Wittenberg et al., 2007; Fox et al.,
290 2008), pixels with an orientation between NW (315°) and NE (45°) were classified as north
291 facing slopes, whereas south facing slopes were classified those that had an orientation
292 between SE (135°) and SW (225°). Pixels within the burn scar not falling within these value
293 ranges were excluded from this type of analysis. All relevant statistical analyses were
294 performed using SPSS v. 18 software package (SPSS Inc., Chicago, IL).

295

296 **5. RESULTS**

297 Firstly the spatio-temporal patterns of vegetation re-growth dynamics established
298 within the whole burn scar and monitored by the NDVI response were evaluated.
299 Subsequently, the influence of topographical parameters on these dynamics was
300 investigated. In regards to the first step, Figure 4 illustrates the NDVI maps area computed
301 for the whole area under the burn scar and Table 1 provides the corresponding descriptive
302 statistics. Furthermore, several NDVI difference maps were produced to assist in evaluating
303 the spatio-temporal changes in NDVI between both before and just after the fire
304 suppression with the post-fire conditions and all subsequent dates (Figure 5).

305 A visual comparison of the pre-fire NDVI with the immediate post-fire NDVI maps
306 (Figure 4a and b) clearly shows the regional extend of the destruction of vegetation caused
307 by the fire. This is further evidenced by the abrupt changes in the descriptive statistics of
308 NDVI under the burnt area, when comparing the pre-fire to post-fire conditions. For
309 example, mean NDVI for the area under the burn scar decreased from 0.499 before the fire
310 to 0.087 after the fire. A decrease in the NDVI maximum value after fire suppression is also
311 noticeable (from 0.789 before the fire to 0.309 after the fire) which shows that some of the

312 vegetation inside the burn scar was only partially destroyed by the fire. In terms of
313 vegetation re-growth dynamics for the area, a visual inspection of the post-fire NDVI maps
314 in combination with the associated NDVI descriptive statistics in Table 1 is indicative of
315 vegetation regeneration taking place in the affected area. Clearly, there is a gradual but
316 steady increase in the maximum and mean NDVI within the fire-affected region towards the
317 pre-fire conditions (Figures 4 and 5), which is indicative of vegetation regeneration in the
318 area. Findings also suggest that during the first two years following the fire suppression,
319 regeneration dynamics were higher in comparison to the subsequent years (Figure 4). Also,
320 as can be observed (Figures 4 and 5), different regeneration dynamics are prevailing within
321 the previously burnt area, with stronger dynamics in regeneration particularly at the centre
322 and west area of the fire-affected region in comparison to the rest of the burnt scar area.

323 In addition, we attempted to fit regression models on the dynamics of the
324 regeneration process. Following other studies (e.g., Hope et al., 2007), scatterplots of the
325 NDVI between pre-fire conditions against subsequent post-fire dates were plotted and
326 slope, intercept and R^2 statistics for the regression line plotted through the data were
327 calculated. Figure 6 illustrates the relevant scatterplots produced and Table 2 summarises
328 the statistics relating to those scatterplots. These data clearly mirror the patterns shown by
329 the NDVI change maps and tables, in that they show a very slow regeneration process.
330 Indeed, the movement of the regression line to back towards the 1:1 line with time is very
331 progressive and gradual, and the increase in R^2 value for the entire burn scar although small
332 is also clear (Table 2).

333 As noted earlier, further analysis was concerned with the investigation of the
334 patterns in vegetation regeneration dynamics - as captured from NDVI- to topographic
335 aspect. Table 3 summarises the descriptive statistics for the NDVI across the whole area
336 under the burn scar separately for the north- and south-facing slopes under the burn scar.
337 Figure 7 also illustrates the spatial variation of the NDVI difference between the pre-fire
338 and most recent to today post-fire TM image separately for the south- and north-facing
339 slopes. In common to the analysis conducted earlier, we also attempted to fit regression
340 models to quantitatively investigate the correlation between post-fire recovery dynamics
341 and aspect. As can be observed from these results (Table 4), the general trajectory of
342 regeneration on north-facing slopes and south-facing slopes also appears to be very slow.
343 Yet, some differences are indeed apparent. A greater level of vegetation destruction is
344 evident on north-facing slopes compared to south-facing slopes and the burnt area in
345 general (a decrease in NDVI of 0.43 on north facing slopes compared to 0.39 on south facing
346 slopes and 0.41 on the burn scar in general). Post-fire regeneration seems to be faster on
347 north-facing slopes in comparison to south-facing slopes. For example, mean NDVI on
348 north-facing slopes increased from 0.09 to 0.30 between July 2007 and July 2009 and then
349 to 0.34 in August 2011, after a very slow period with no real increase in NDVI between July
350 2009 and August 2010. On south facing slopes the increase appears lower, from 0.09 to 0.22
351 between July 2007 and July 2009 and then to 0.25 in August 2011. The percentage increase
352 in regenerated vegetation by August 2010 was similar on north- and south-facing slopes. On
353 the north-facing and south-facing subsets, the highest regeneration was observed in the
354 period immediately following the fire (July 2007-July 2009). After very slow (if not
355 negligible) regeneration between July 2009 and August 2010, the rate of vegetation
356 regeneration then increased during the most recent time period. These data also confirm
357 the faster regeneration on north-facing slopes compared to south-facing slopes, with higher
358 slopes and R^2 values in all cases (R^2 values of scatterplots on north-facing slopes were
359 double that of south-facing slopes for the two most recent time intervals).

360

361

6. DISCUSSION

362

The results presented here indicate the large degree of spatial variability in terms of vegetation regeneration in the study region. They also underline the significance of wildfires such as that occurred on Mt. Parnitha as agents of vegetation destruction and modifiers of the landscape. Results also clearly show that vegetation regeneration in the affected area is a process that can potentially take a long time. Indeed, four years after the fire the landscape had still not reached pre-fire vegetation coverage; in fact NDVI levels had only just passed half their original pre-fire levels. This is in common with previous studies of the fire regeneration of vegetation on Mount Parnitha and Mount Taygetos in Greece (Arianoutsou et al., 2010). Yet, those contrast those reported by Wittenberg et al., (2007) who showed that vegetation had recovered to pre-fire conditions within five years in Mount Carmel, Israel, even following multiple fires. The fact that the greatest regeneration was observed during a two year interval may be significant when comparing to lower regeneration during subsequent time intervals which were only one year long, or this pattern could reflect the rapid regrowth of vegetation immediately following the fire, and more gradual vegetation regrowth during subsequent periods as soil and hydrological characteristics improved.

363

Arianoutsou et al (2010) found that the recovery for tree species (*Abies cephalonia* and *Pinus nigra*) was likely to be slow in general, with some localised differences in common with fire-disturbed ecosystems elsewhere in the Mediterranean (Southern Spain – Clemente et al., 2006 and Mayor et al., 2007; Portugal - Gouveia et al., 2010), in the United States (Chen et al., 2011) and Indonesian Borneo (Hoscilo et al, 2013). The concentration of dark green regions (indicating higher NDVI) in the central areas of the burn scar region in 2009, 2010 and 2011 (Figure 4) and the orange and red areas in Figure 5 and Figure 7 (indicating greater regeneration) indicate that vegetation regeneration was focused to a greater extent on these areas. This point to a spatial heterogeneity in vegetation and landscape response as a result of more localized factors. This more complex pattern of vegetation regeneration is also in good agreement with many studies (e.g. Inbar et al., 1998) reporting very fast regeneration rates within the first two years following wildfires and many other authors finding that regeneration was faster on north-facing slopes compared to south-facing slopes (e.g. Inbar et al., 1998; Pausas and Vallejo, 1999; Cerdá and Doerr, 2005; Fox et al., 2008).

364

Many studies (e.g. Gouveia et al., 2008, 2009) have identified that water availability is a major limiting factor on fire frequency and regeneration because vegetation is generally more dense in wetter areas compared to drier areas (Gouveia et al., 2010). In Greece, as well as the wider Mediterranean region, some studies suggest that hydrological changes (e.g. more frequent droughts) could lead to an increased frequency of fires similar to that of June 2007 and that forest fires are increasingly occurring in higher latitude areas and at higher altitudes, where the forest species, in contrast to those growing at lower altitudes and latitudes in the Mediterranean regions, have not developed a regenerative response to regular disturbance by fire (Arianoutsou et al., 2010; Retana et al., 2012). If this is the case, then it is likely that it will be increasingly difficult for landscapes to recover to pre-fire conditions as the recovery process has been shown to be relatively long. As the present work has shown, the Mt. Parnitha burn scar area had not recovered to half its pre-fire vegetation levels within four years. If this region suffered further fires, then the resilience and sustainability of this economically and culturally valuable ecosystem would inevitably be threatened as has been shown in other regions of Greece (Christakopoulos et al., 2007).

408 One of the key factors that need to be considered when planning for the effects of
409 such wildfires is the species composition of the ecosystems. Ganatsas et al., (2012) and
410 Arianoutsou et al., (2010) have both demonstrated that the slow regeneration of vegetation
411 (especially *A. cephalonia*) on the burn scar in Mt. Parnitha is, in part, due to the fact that they
412 are obligate seeders whose seeds ripen in August. These seeds may be destroyed during
413 summer wildfires and as such will not be able to regenerate. Ecosystem recovery in forests
414 dominated by these species is then likely to be dominated by scrubland species, rather than
415 the original forest species. This pattern was observed by Crotteau et al., (2013) in the
416 southern Cascades, USA, where regions which had high-severity burns were dominated by
417 greater shrub coverage. Puerta-Piñero et al. (2010) showed that long-standing, stable forest
418 areas display faster regeneration than younger forests. The implications of this for the long
419 term sustainability of these types of ecosystems in a future of more frequent fires are
420 significant since forests may not be allowed the time to develop into stable communities that
421 are able to recover quickly. The resilience of these ecosystems, will, therefore, be
422 significantly reduced under a regime of increased fire frequency (Díaz-Delgado et al., 2002).

423 In common with analogous studies conducted elsewhere (e.g. on the Iberian
424 Peninsula – Pausas and Vallejo, 1999, Cerdá and Doerr, 2005; SE France – Fox et al., 2008;
425 Mt. Carmel, Israel - Kutiel, 1994, Inbar et al. 1998; Wittenberg et al. 2007) it is also clear that
426 aspect is a key control on the rate of vegetation regeneration. It is likely that this reflects the
427 local effects of microclimate on hydrological processes which play an important role in
428 triggering vegetation re-growth. Such differences in post-fire regeneration can both reflect
429 and influence localised hydrological variability through soil hydrophobicity (Cerdá and
430 Doerr, 2005) and changes in overland flow patterns and soil erosion, especially through
431 destroying protective vegetation and litter on the forest floor (Shakesby and Doerr, 2006).
432 Mayor et al., (2007) showed that sediment yield and runoff in an unburned catchment in
433 Spain were considerably less than in burned catchments, for six years following a wildfire. In
434 small, upland catchments in particular, this may have significant impacts on flood risk.

435 This study has focused on changes in land cover over a relatively short period (2007-
436 2011). However, it is recognised that post-fire ecosystem recovery is historically contingent
437 and can be a function of pre-fire forest cover, land-use, species composition and fire history
438 (Gouveia et al., 2010; Puerta-Piñero et al., 2010) and more long term land cover and fire
439 history is needed in order to fully understand ecosystem dynamics (Chen et al., 2011).
440 Analysis of historical maps, aerial photography and other documentary evidence may
441 augment the high resolution spatial data provided by EO data. Historical reconstructions,
442 similar to that performed by Korb et al., (2012) in south west Colorado, USA, can be
443 particularly useful when compared with more recent data. One of the principal areas in which
444 EO could be deployed in this field is through the remote sensing of soil moisture (Bourgeau-
445 Chavez et al., 2007). In addition, it would be instructive to complement the inter-annual
446 measurements of regeneration provided by EO data with intra-annual and seasonal data in
447 order to provide a more complete picture of land cover dynamics following wildfires
448 (Lhermitte et al., 2011). At this point, it is also worthwhile to note that it was not possible to
449 quantify uncertainties in the DEM used to derive the topographical information for the study
450 area (elevation, slope, aspect), and included herein. As such, potential inaccuracies in the
451 predictions of these parameters and their relationships to the ecosystem recovery dynamics
452 identified in the area could not be incorporated in the analysis and the results
453 interpretation. Results are, however, in line with other studies examining the relationships
454 between post-fire vegetation recovery and topographic parameters (Díaz-Delgado et al.,

455 2003; Wittenberg et al., 2007; Fox et al., 2008), which also did not conduct any kind of
456 analysis to examine such relationships.

457 Accurate assessments of vegetation recovery in burnt areas requires not only a
458 qualitative analysis (species, communities), but also the determination of abundance
459 (vegetation cover, Leaf Area Index, biomass). The results of this study imply that routine
460 assessment of a restoration process can be possible from the synergy of EO and GIS,
461 providing that suitable imagery is available at no cost and at regular time intervals. As
462 wildfires in Mediterranean areas and similar ecosystems across the globe are causing
463 significant changes to land cover and pose a serious threat to ecosystem resilience, the
464 complex, multi-scale cooperation required to effectively plan for, and manage the effects of
465 these fires (described by Morehouse et al., 2011) can be aided by the use of EO data such as
466 Landsat data. Such analysis, should, evidently, be combined with ground-truthed high-
467 resolution (both spatial and temporal) ecological surveys wherever possible. Images
468 acquired at annual (or even sub-annual) resolution would be ideal as it would enable us to
469 adequately factor seasonal and phenological factors in to the analyses. Such analyses would
470 allow us to obtain a more detailed understanding of the response of such critical ecosystems
471 to disturbance by fire. In a future of increased wildfire frequency as a result of climate
472 change, such information is essential for ensuring landscape and ecosystem sustainability.

473 In conclusion, it should be noted that the present study has focused on exploring
474 vegetation re-growth based on the use of NDVI but without distinguishing between different
475 vegetation types in the regeneration dynamics. This can be considered as a downside of the
476 approach followed herein, given that knowledge of vegetation types and conditions is
477 required to better understand and interpret the nature of the wildland fire damage (Milne,
478 1986). Yet, NDVI is a parameter that can provide information on vegetation green biomass
479 amount, which essentially is what is needed when decision need to be taken in forest
480 management and planning, thus making it a very useful tool from a practical point of view
481 (Malak and Pausas, 2006). Furthermore, it will be interesting in future work to explore the
482 spatio-temporal relationships of vegetation re-growth with other factors, such as the type of
483 the actual fuel burnt, slope angle or soil type.

484

485 **7. CONCLUSIONS**

486 In this study an analysis of vegetation recovery dynamics in a Mediterranean
487 ecosystem of high environmental and socio-economical importance impacted by a
488 significant wildfire based on the analysis of multiple Landsat TM images was presented.
489 These EO data were integrated in a GIS framework to enable the analysis of changes in NDVI
490 on a burn scar on Mount Parnitha, Greece, on four dates following the fire that occurred on
491 June 2007. These changes enabled us to assess the regeneration of the ecosystem after the
492 fire and to also explore the spatio-temporal variation of vegetation regeneration dynamics
493 in respect to topographic aspect.

494 Results suggested a very slow post-fire recovery, with the post-fire NDVI spatial
495 pattern showing a relatively rapid regeneration in the two years following the fire, but
496 becoming more gradual in subsequent years. It appears that vegetation in the fire-affected
497 area has not yet reached pre-fire conditions and results suggest that it may take a number
498 of years for this to occur. Interestingly, results suggested as well that north-facing slopes
499 exhibited a slightly faster rate of recovery compared to south-facing slopes. This might be
500 due to more favourable micro-climatic and hydrological conditions for vegetation growth in
501 these areas. In this respect, similar findings have been reported by other investigators

502 examining the effect of topography on post-fire vegetation regeneration in Mediterranean
503 ecosystems and elsewhere.

504 An understanding of the spatial patterns of vegetation re-growth dynamics in fire-
505 affected areas can assist to better appreciate post-fire landscape processes, which can
506 subsequently aid restoration actions in the affected region. In addition, the present study
507 contributes to the understanding of Mediterranean landscape dynamics, and corroborates
508 the usefulness of NDVI in post-fire regeneration assessment. Last but not least, it confirms
509 that EO technology and GIS analysis techniques can provide a potentially operational
510 solution to support local studies of land cover restoration after wildfires, provided that
511 satellite imagery can be acquired at regular time intervals over a given region.

512

513 **Acknowledgments**

514 Authors wish to thank the United States Geological Survey (USGS) for the free
515 access to the Landsat TM satellite images. Dr. Petropoulos is thankful to the Greek
516 Scholarships Foundation (IKY) for supporting this work. Authors also express thanks Mr.
517 Anthony Smith from Aberystwyth University for his help with the figures preparation
518 included in the manuscript.

519

520

521

521 **REFERENCES**

522 Arianoutsou, M., Christopoulou, A., Kazanis, D., Tountas Th, G. E., Bazos, I., & Kokkoris, Y.
523 (2010). Effects of fire on high altitude coniferous forests of Greece. In *6th*
524 *international conference of wildland fire, Coimbra*.

525 ASTER GDEM (2009). ASTER GDEM Version. 1. Readme File <http://www.gdem.aster.ersdac.or.jp> [accessed on July 24th, 2011].

527 Bisson, M., Fornaciai, A., Coli, A., Mazzarini, F., & Pareschi, M. T. (2008). The vegetation
528 resilience after fire (VRAF) index: development, implementation and an illustration
529 from central Italy. *International Journal of Applied Earth Observation and*
530 *Geoinformation*, 10(3), 312-329.

531 Bourgeau-Chavez, L. L., E. S. Kasischke, K. Riordan, S. Brunzell, M. Nolan, E. Hyer, J.
532 Slawski, M. Medvecz, T. Walters, & S. Ames (2007). Remote monitoring of spatial and
533 temporal surface soil moisture in fire disturbed boreal forest ecosystems with ERS
534 SAR imagery. *International Journal of Remote Sensing* 28 (10), 2133-2162.

535 Casady, G.M., W.J.D. Leeuwen, S.E. Marsh (2009). Evaluating post-wildfire vegetation
536 regeneration as a response to multiple environmental determinants. *Environmental*
537 *Model Assessment*, 15 (5), 295-307.

538 Cerdá, A., & Doerr, S. H. (2005). Influence of vegetation recovery on soil hydrology and
539 erodibility following fire: an 11-year investigation. *International Journal of Wildland*
540 *Fire*, 14(4), 423-437.

541 Chen, S. S., Chen, L. F., Liu, Q. H., Li, X., & Tan, Q. (2005). Remote sensing and GIS-based
542 integrated analysis of coastal changes and their environmental impacts in Lingding
543 Bay, Pearl River Estuary, South China. *Ocean & coastal management*, 48(1), 65-83.

544 Chen, X., Vogelmann, J. E., Rollins, M., Ohlen, D., Key, C. H., Yang, L., Huang, C. & Shi, H.
545 (2011). Detecting post-fire burn severity and vegetation recovery using
546 multitemporal remote sensing spectral indices and field-collected composite burn
547 index data in a ponderosa pine forest. *International Journal of Remote*
548 *Sensing*, 32(23), 7905-7927.

- 549 Christakopoulos, P., Hatzopoulos, I., Kalabokidis, K., Paronis, D., & Filintas, A. (2007)
550 Assessment of the response of a Mediterranean-type forest ecosystem to recurrent
551 wildfires and to different restoration practices using Remote Sensing and GIS
552 techniques. *Proceedings of the 6th international workshop of the EARSEL special*
553 *interest group on forest fires*, 213-216.
- 554 Clemente, R. H., Cerrillo, R. M., Bermejo, J. E., & Gitas, I. Z. (2006). Modelling and
555 monitoring post-fire vegetation recovery and diversity dynamics: A diachronic
556 approach using satellite time-series data set. *Forest ecology and management*, 234,
557 S194.
- 558 Crotteau, J. S., Varner III, M., & Ritchie, M. W. (2013). Post-fire regeneration across a fire
559 severity gradient in the southern Cascades. *Forest Ecology and Management*, 287,
560 103-112.
- 561 Díaz-Delgado R., Lloret F, Pons X., & Terradas J. (2002). Satellite evidence of decreasing
562 resilience in Mediterranean plant communities after recurrent wildfires. *Ecology*, 83,
563 2293-2303.
- 564 Diaz-Delgado, R., Lloret, F., & Pons, X. (2003). Influence of fire severity on plant
565 regeneration through remote sensing imagery. *International Journal of Remote*
566 *Sensing*, 24(8), 1751-1763.
- 567 Durduran, S.S. (2010). Coastline change assessment on water reservoirs located in the
568 Konya Basin Area, Turkey, using multitemporal Landsat imagery, *Environmental*
569 *Monitoring and Assessment*, 164, 453-461.
- 570 Elvira, L.M., & Hernando, C. (1989). Inflamabilidad y energia de las especies de
571 sotobosque (estudio piloto con aplicación a los incendios forestales). Monografias
572 INIA nº 68, Ministerio de Agricultura Pesca y Alimentacion. Madrid.
- 573 Fox, D. M., Maselli, F., & Carrega, P. (2008). Using SPOT images and field sampling to map
574 burn severity and vegetation factors affecting post forest fire erosion risk. *Catena*,
575 75(3), 326-335.
- 576 Ganatsas, P., Daskalakou, E., & Paitaridou, D. (2012). First results on early post-fire
577 succession in an *Abies cephalonica* forest (Parnitha National Park, Greece). *iForest-*
578 *Biogeosciences and Forestry*, 5(1), 6.
- 579 Gens, R. (2010). Remote sensing of coastlines: detection, extraction and monitoring.
580 *International Journal of Remote Sensing*, 31(7), 1819-1836.
- 581 Gouveia, C., DaCamara, C. C., & Trigo, R. M. (2010). Post-fire vegetation recovery in
582 Portugal based on spot/vegetation data. *Natural Hazards and Earth System Science*,
583 10(4), 673-684
- 584 Gouveia, C., Trigo, R. M., & DaCamara, C. C. (2009). Drought and vegetation stress
585 monitoring in Portugal using satellite data. *Natural Hazards and Earth System*
586 *Science*, 9(1), 185-195.
- 587 Gouveia, C., Trigo, R. M., DaCamara, C. C., Libonati, R., & Pereira, J. M. C. (2008). The North
588 Atlantic Oscillation and European Vegetation Dynamics, *Int. J. Climatol.*, 28(14),
589 1835-1847.
- 590 Grissino-Mayer, H. D., & Swetnam, T. W. (2000). Century-scale climate forcing of fire
591 regimes in the American Southwest. *Holocene*, 10(2), 213-220.
- 592 Hall, F., Botkin, D., Strebel, D., Woods, K., & Goetz, S. (1991). Large-scale patterns of forest
593 succession as determined by remote sensing. *Ecology*, 72, 628-640.

- 594 Hope, A., Tague, C., & Clark, R. (2007). Characterizing post-fire vegetation recovery of
595 California chaparral using TM/ETM+ time-series data. *International Journal of*
596 *Remote Sensing*, 28(6), 1339-1354.
- 597 Hoschilo, A., Tansey, K. J., & Page, S. E. (2013). Post-fire vegetation response as a proxy to
598 quantify the magnitude of burn severity in tropical peatland. *International Journal of*
599 *Remote Sensing*, 34(2), 412-433.
- 600 Inbar, M., Tamir, M., & Wittenberg, L. (1998). Runoff and erosion processes after a forest
601 fire in Mount Carmel, a Mediterranean area. *Geomorphology*, 24(1), 17-33.
- 602 Irons, J. 2011. Landsat 7 science data user's handbook, Report 430-15-01-003-0. National
603 Aeronautics and Space Administration, <http://landsathandbook.gsfc.nasa.gov/>
604 [accessed on July 10th, 2013].
- 605 Jakubauskas, M. E., Lulla, K. P., & Mausel, P. W. (1990). Assessment of vegetation change
606 in a fire-altered forest landscape. *PE&RS, Photogrammetric Engineering & Remote*
607 *Sensing*, 56(3), 371-377.
- 608 Jensen, J. R., (2000). *Remote Sensing of the Environment: An Earth Resource Perspective*.
609 Saddle River, N.J, Prentice Hall:.
- 610 Justice, C.O., Malingreau, J.P., & Setzer, A.W., (1993). Satellite remote sensing of fire:
611 potential and limitation. In: Crutzen, P., & Goldammer, J. (Eds.), *Fire in the*
612 *Environmental: The Ecological, Atmospheric, and Climatic Importance of Vegetation*
613 *Fires* (pp. 77-88.). New York, John Wiley and Sons
- 614 Kalivas, D., Petropoulos, G.P., Athanasiou, I. % V. Kollias (2013). An intercomparison of
615 burnt area estimates derived from key operational products: analysis of Greek
616 wildland fires 2005-2007. *Nonlinear Processes in Geophysics*, 20, 1-13.
- 617 Keeley, J. E. (2000). Chaparral. In: M. G. Barbour, & W. D. Billings (Eds.), *North American*
618 *terrestrial vegetation* (pp. 204-253). New York: Cambridge University Press.
- 619 Kokaly, R. F., Rockwell, B. W., Haire, S. L., & King, T. V. (2007). Characterization of post-fire
620 surface cover, soils, and burn severity at the Cerro Grande Fire, New Mexico, using
621 hyperspectral and multispectral remote sensing. *Remote Sensing of*
622 *Environment*, 106(3), 305-325.
- 623 Korb, J. E., Fulé, P. Z., & Stoddard, M. T. (2012). Forest restoration in a surface fire-
624 dependent ecosystem: An example from a mixed conifer forest, southwestern
625 Colorado, USA. *Forest Ecology and Management*, 269, 10-18.
- 626 Kutiel, P. (1994). Fire and ecosystem heterogeneity: a Mediterranean case study. *Earth*
627 *Surface Processes and Landforms*, 19(2), 187-194.
- 628 Latifovic, R., Fytas, K., Chen, J. & Paraszczak, J., (2005). Assessing land cover change
629 resulting from large surface mining development, *International Journal of Applied*
630 *Earth Observation and Geoinformation*, 7(1), 29-48.
- 631 Le Houérou, H. N., Bingham, R. L., & Skerbek, W. (1988). Relationship between the
632 variability of primary production and the variability of annual precipitation in world
633 arid lands. *Journal of arid Environments*, 15(1), 1-18.
- 634 Lhermitte, S., Verbesselt, J., Verstraeten, W. W., Veraverbeke, S., & Coppin, P. (2011).
635 Assessing intra-annual vegetation regrowth after fire using the pixel based
636 regeneration index. *ISPRS Journal of Photogrammetry and Remote Sensing*, 66(1), 17-
637 27.
- 638 Lillesand T. M. & Kiefer R. W., (2000). *Remote Sensing and Image Interpretation*, (4th ed.),
639 Chichester, Wiley & Sons.

- 640 Malak, D A., and J. G. Pausas (2006). Fire regime and post-fire Normalised Difference
641 Vegetation Index changes in the eastern Iberian peninsula (Mediterranean basin).
642 *Intern. Journal of Wildland Fire*, 15, 407-413.
- 643 Mayor, A. G., Bautista, S., Llovet, J., & Bellot, J. (2007). Post-fire hydrological and erosional
644 responses of a Mediterranean landscape: Seven years of catchment-scale dynamics.
645 *Catena*, 71(1), 68-75.
- 646 Millán, M.M., Estrela, M.J., & Caseller, V., 1995. Torrential precipitations on the Spanish
647 east coast: the role of the Mediterranean sea surface temperature. *Atmos. Res.* 36, 1-
648 16.
- 649 Milne, A.K. (1986). The use of remote sensing in mapping and monitoring vegetational
650 change associated with bushfire events in eastern Australia. *Geocarto International*,
651 1, 25-32.
- 652 Minchella, A., F. Del Frate, F. Capogna, S. Anselmi, F. Manes (2009). Use of multitemporal
653 SAR data for monitoring vegetation recovery of Mediterranean burned areas. *Remote*
654 *Sensing and Environment*, 113(3), 588-597.
- 655 Morehouse, B. J., Henderson, M., Kalabokidis, K., & Iosifides, T. (2011). Wildland Fire
656 Governance: Perspectives from Greece. *Journal of Environmental Policy & Planning*,
657 13(4), 349-371.
- 658 Mouillot, F., Ratte, J. P., Joffre, R., Mouillot, D., & Rambal, S. (2005). Long-term forest
659 dynamic after land abandonment in a fire prone Mediterranean landscape (central
660 Corsica, France). *Landscape Ecology*, 20(1), 101-112.
- 661 National Oceanic and Atmospheric Administration (NOAA), 2007.
662 [http://www.ncdc.noaa.gov/cdo-](http://www.ncdc.noaa.gov/cdo-web/datasets/GHCNDMS/stations/GHCND:GR000016716/detail)
663 [web/datasets/GHCNDMS/stations/GHCND:GR000016716/detail](http://www.ncdc.noaa.gov/cdo-web/datasets/GHCNDMS/stations/GHCND:GR000016716/detail) [accessed on
664 October 4th, 2013].
- 665 Naveh, Z. (1974). Effects of fire in Mediterranean Region. In: Kozlowsky, T.T., Ahlgren,
666 C.E. (Eds.), *Fire Ecosystems* (pp. 401-434.), New York, Academic Press,
- 667 Otukei, J. R., & Blaschke, T. (2010). Land cover change assessment using decision trees,
668 support vector machines and maximum likelihood classification algorithms.
669 *International Journal of Applied Earth Observation and Geoinformation*, 12, S27-S31.
- 670 Pausas J.G., Ribeiro E., & Vallejo, R. (2004). Post-fire regeneration variability of *Pinus*
671 *halepensis* in the eastern Iberian Peninsula. *For Ecol Manag* 203,251-259.
- 672 Pausas, J. G., & Vallejo, V. R. (1999). The role of fire in European Mediterranean
673 ecosystems. In Chivieco, C. (Ed.) *Remote Sensing of Large Wildfires in the European*
674 *Mediterranean Basin* (pp. 3-16), Berlin Heidelberg Springer..
- 675 Pereira, J. M., Sá, A. C., Sousa, A. M., Silva, J. M., Santos, T. N., & Carreiras, J. M. (1999).
676 Spectral characterization and discrimination of burnt areas. In: Chuvieco (Eds.),
677 *Remote Sensing of Large Wildfires in the European Mediterranean Basin*. Springer-
678 Verlag, Berlin/Heidelberg, pp. 122-138.
- 679 Petropoulos G.P. and C. Kalaitzidis (2011). Multispectral vegetation indices in remote
680 sensing: an overview – book chapter. In “Ecological Modeling”, Chapter 2, 15-39,
681 Novapublishers, USA, ISBN: 978-1-61324-567-5
- 682 Petropoulos, G., K.P. Vadrevu, G. Xanthopoulos, G., Karantounias and M. Scholze (2010). A
683 Comparison of Spectral Angle Mapper and Artificial Neural Network Classifiers
684 Combined with Landsat TM Imagery Analysis for Obtaining Burnt Area Mapping.
685 *Sensors*, 10, 1967-1985.
- 686 Petropoulos, G. P., Kontoes, C., & Keramitsoglou, I. (2011). Burnt area delineation from a
687 uni-temporal perspective based on Landsat TM imagery classification using Support

688 Vector Machines. *International Journal of Applied Earth Observation and*
689 *Geoinformation*, 13(1), 70-80.

690 Petropoulos, G.P., C. C. Kontoes, and I. Keramitsoglou (2012). Land cover mapping with
691 emphasis to burnt area delineation using co-orbital ALI and Landsat TM imagery.
692 *International Journal of Applied Earth Observation and Geoinformation*, 18, 344-355.

693 Politi, P. I., Arianoutsou, M., & Stamou, G. P. (2009). Patterns of *Abies cephalonica* seedling
694 recruitment in Mount Aenos National Park, Cephalonia, Greece. *Forest Ecology and*
695 *Management*, 258(7), 1129-1136.

696 Puerta-Piñero, C., Sánchez-Miranda, A., Leverkus, A., & Castro, J. (2010). Management of
697 burnt wood after fire affects post-dispersal acorn predation. *Forest Ecology and*
698 *Management*, 260(3), 345-352.

699 Quintano, C., Fernandez-Manso, A., Fernandez-Manso, O., & Shimabukuro, Y.E., (2006).
700 Mapping burnt areas in Mediterranean countries using spectral mixture analysis
701 from a uni-temporal perspective. *International Journal of Remote Sensing*, 27, 4, 645-
702 662.

703 Retana, J., Arnan, X., Arianoutsou, M., Barbati, A., Kazanis, D., & Rodrigo, A. (2012). Post-
704 fire management of non-serotinous pine forests. In Moreira, F., Arianoutsou, M.,
705 Corona, P., & De las Heras, J. (Eds.). *Post-Fire Management and Restoration of Southern*
706 *European Forests* (pp. 151-170). Netherlands, Springer..

707 Roder, A., Hill, J., Duguay, B., Alloza, J. A., & Vallejo, R. (2008). Using long time series of
708 Landsat data to monitor fire events and postfire dynamics and identify driving
709 factors. A case study in the Ayora region (eastern Spain), *Remote Sens. Environ.*, 112,
710 259– 273.

711 Rouse, J.W., Haas, R.H., Schell, J.A. & Deering, D.W., 1973, Monitoring vegetation systems
712 in the Great Plains with ERTS. In *3rd ERTS Symposium*, NASA SP-351 I, pp. 309–317.

713 Schmidt, H., & Glasser, C., (1998). Multitemporal analysis of satellite data and their use in
714 the monitoring of the environmental impacts of open cast lignite mining areas in
715 eastern Germany. *International Journal of Remote Sensing* 19, 2245–2260.

716 Segah, H., Tani, H. & Hirano, T. (2010). Detection of fire impact and vegetation recovery
717 over tropical peat swamp forest by satellite data and ground-based NDVI instrument.
718 *International Journal of Remote Sensing*, 31 (20), 5297-5314.

719 Shakesby, R.A., & Doerr, S.H., 2006. Wildfire as a hydrological and geomorphological
720 agent. *Earth-Science Reviews* 74, 269–307.

721 Smith, A.M.S, Drake, N.A., Wooster, M.J., Hudak, A.T., Holden, Z.A., & Gibbons, C.J., (2007).
722 Production of Landsat ETM+ reference imagery of burnt areas within Southern
723 African savannahs: comparison of methods and application to MODIS. *International*
724 *Journal of Remote Sensing*, 28, 12, 2753-2775.

725 Solans Vila J.P. & Barbosa P. (2010). Post-fire vegetation regrowth detection in the Deiva
726 Marina region (Liguria-Italy) using Landsat TM and ETM+ data. *Ecological Modelling*
727 2121 p.75–84.

728 Steyaert, L., Hall, F., & Loveland, T., (1997). Land cover mapping, fire regeneration, and
729 scaling studies in the Canadian boreal forest with 1 km AVHRR and Landsat TM data.
730 *International Journal of Geophysical Research* 102, 29581–29598.

731 Stueve, K., Cerney, D., Rochefort, R., & Kurt, L., (2009). Post-fire tree establishment
732 patterns at the alpine treeline ecotone: Mount Rainier National Park, Washington,
733 USA. *Journal of Vegetation Science*, 20, 107–120.

734 Sunee, S., Hussin, Y. A., & de Gier, A. (2001). Assessment of forest recovery after fire using
735 Landsat TM images and GIS techniques: a case study of Mae Wong national park,

736 Thailand. In *ACRS Proceedings of the 22nd Asian Conference on Remote Sensing ACRS,*
737 *Singapore.*

738 Vapnik, V. (1995): *The nature of statistical learning theory*, New York, NY: Springer-
739 Verlag.

740 Veraverbeke, S., Somers, B., Gitas, I., Katagis, T., Polychronaki, A., & Goossens, R. (2012).
741 Spectral mixture analysis to assess post-fire vegetation regeneration using Landsat
742 Thematic Mapper imagery: accounting for soil brightness variation. *International*
743 *Journal of Applied Earth Observation and Geoinformation*, 14(1), 1-11.

744 Veraverbeke, S., W. W. Verstraeten, S. Lhermitte & R. Goossens (2010). Evaluating
745 Landsat Thematic Mapper spectral indices for estimating burn severity of the 2007
746 Peloponnese wildfires in Greece. *International Journal of Wildland fire*, 19, 558-569.

747 Viedma, O., Meliá, J., Segarra, D., & García-Haro, J. (1997). Modeling rates of ecosystem
748 recovery after fires by using Landsat TM data. *Remote Sensing of Environment*, 61,
749 383-398.

750 White, J.D., K.C. Ryan, C.C. Key, & S.W. Running, (1996). Remote sensing of forest fire
751 severity and vegetation recovery. *International Journal of Wildland Fire*, 6(3):125-
752 136.

753 Wittenberg, L., Malkinson, D., Beerli, O., Halutzy, A., & Tesler, N. (2007). Spatial and
754 temporal patterns of vegetation recovery following sequences of forest fires in a
755 Mediterranean landscape, Mt. Carmel Israel. *Catena*, 71(1), 76-83.

756

Subject: Research Highlights of submitted paper

1. Investigate ecosystem recovery dynamics following a fire event occurred in a Mediterranean region, exploiting free distributed EO imagery and GIS analysis techniques.
2. Explore the spatio-temporal relationships of re-growth dynamics under the burn scar to topographical characteristics of the fire-affected area.
3. Findings can be helpful in restoration efforts taking place in the affected area, that being a setting of high ecological, environmental and cultural importance for the local community and not only.
4. Our work contributes to the understanding Mediterranean landscape dynamics, and corroborates the practical usefulness of EO technology and GIS as an effective tool in policy decision making and successful landscape management, potentially as an operation service solution.

List of Figures:

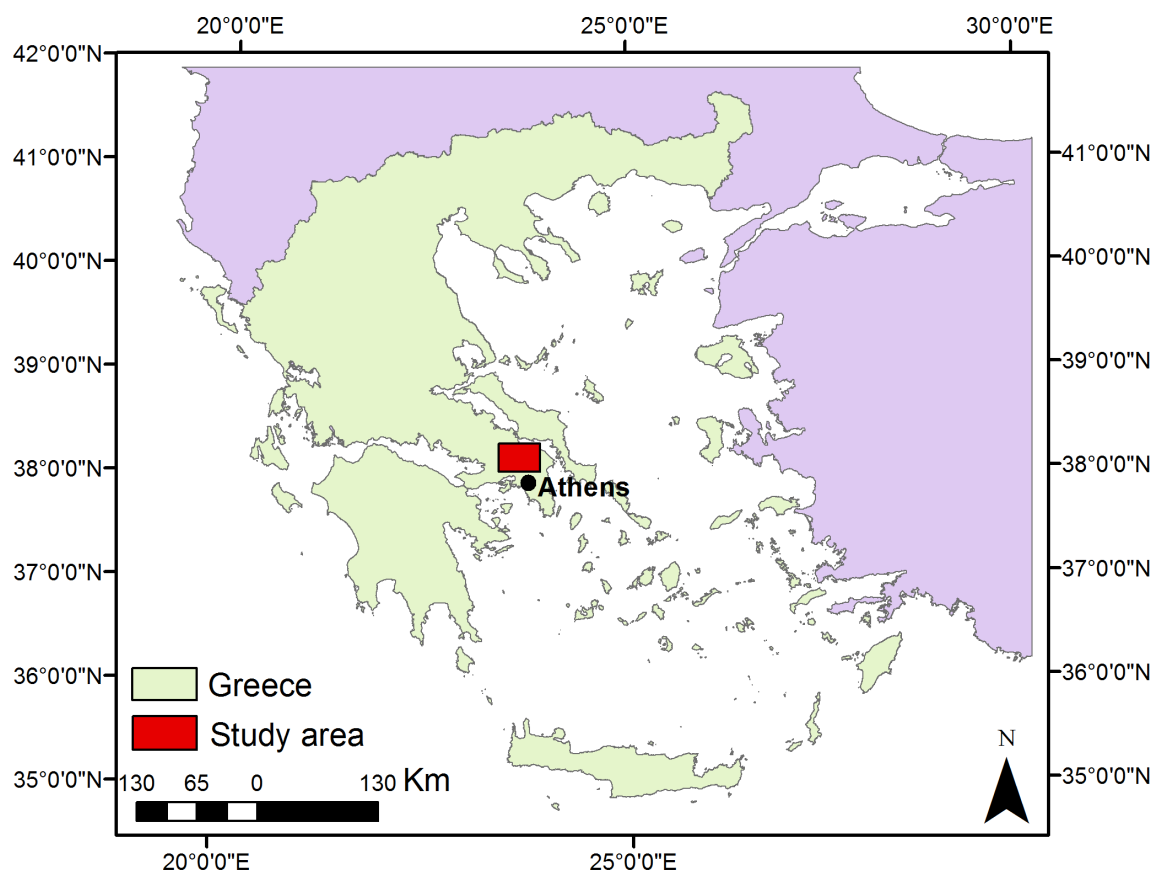


Figure 1: Study area location in Greece (indicated by the red colored box)

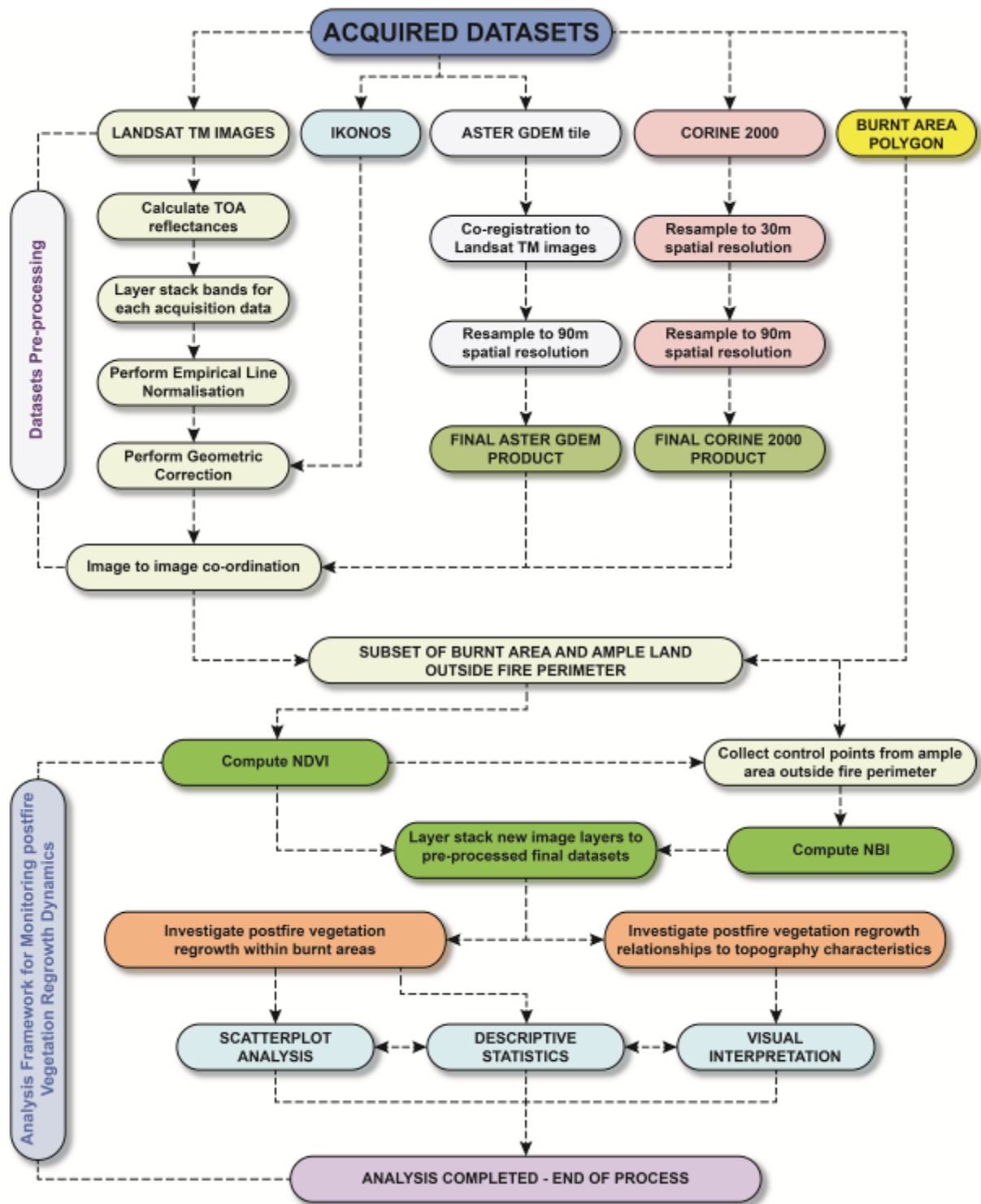


Figure 2: Overall methodology implemented in our study for analyzing the regrowth dynamics of the studied region using the TM data.

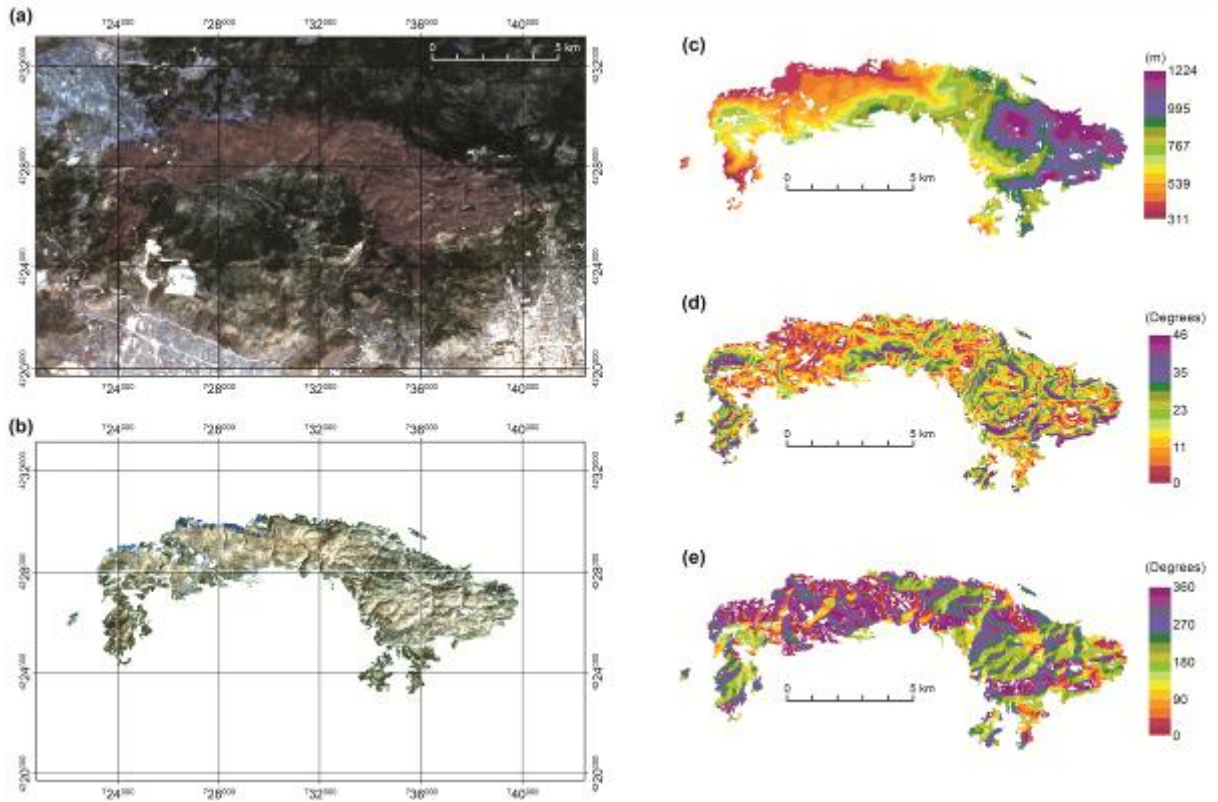


Figure 3: An illustration of some key datasets derived upon completion of the pre-processing steps. From left to right: a) the initial subset of the study area on the TM image acquired on July 3rd, 2000, (b) the masked area inside the burnt area envelope for the same image, (c) elevation and (d) aspect maps of the area covered by the burnt area envelop derived from ASTER Global Digital Elevation (GDEM) product.

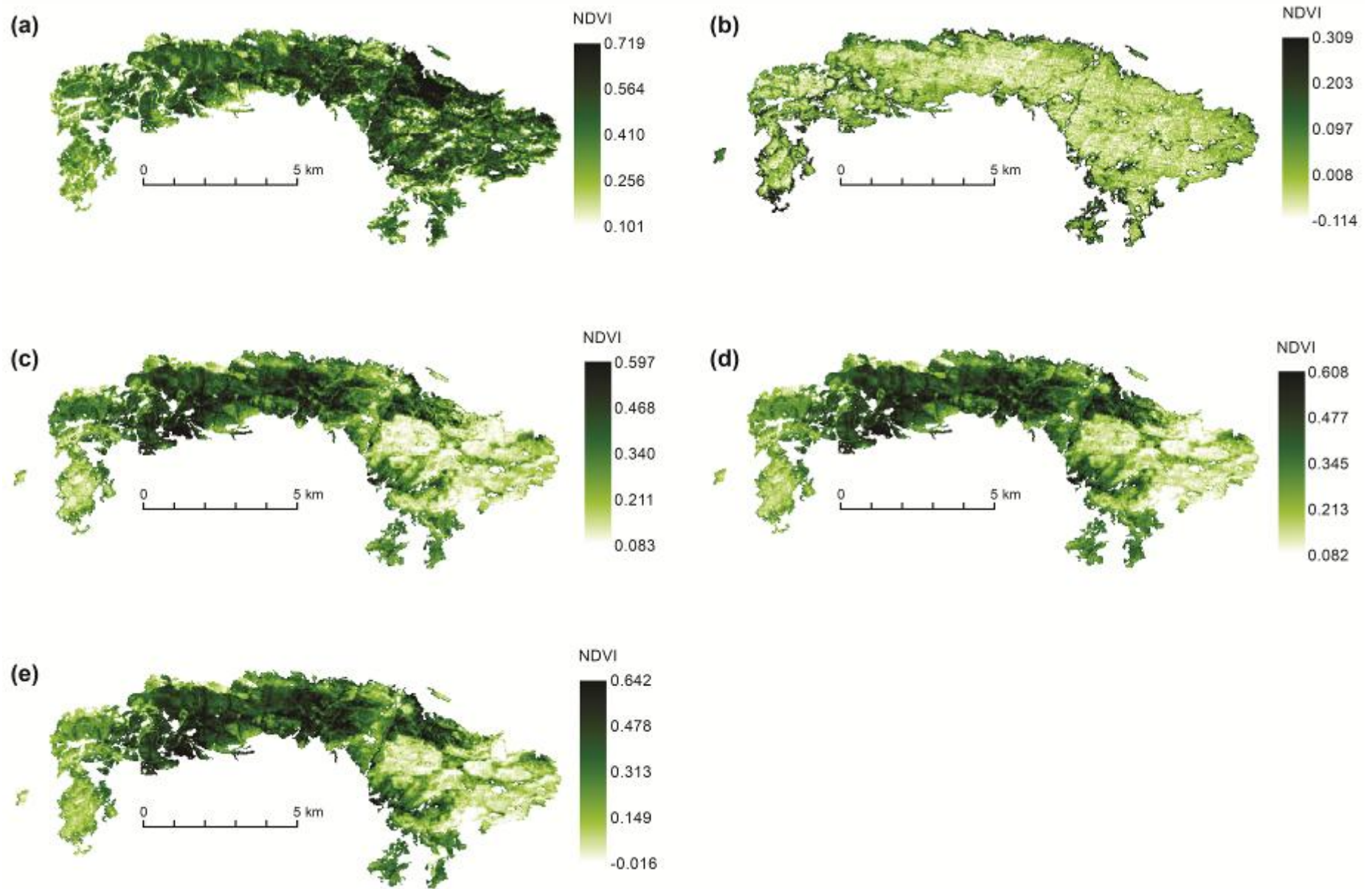


Figure 4: NDVI maps computed from the pre-processed Landsat TM images: (a) May 16th, 2007, (b) July 3^d, 2007, (c) July 24, 2009, (d) August 13th, 2010 & (e) August 15th, 2011. The variation in the NDVI ranges between the different days of observation is evident.

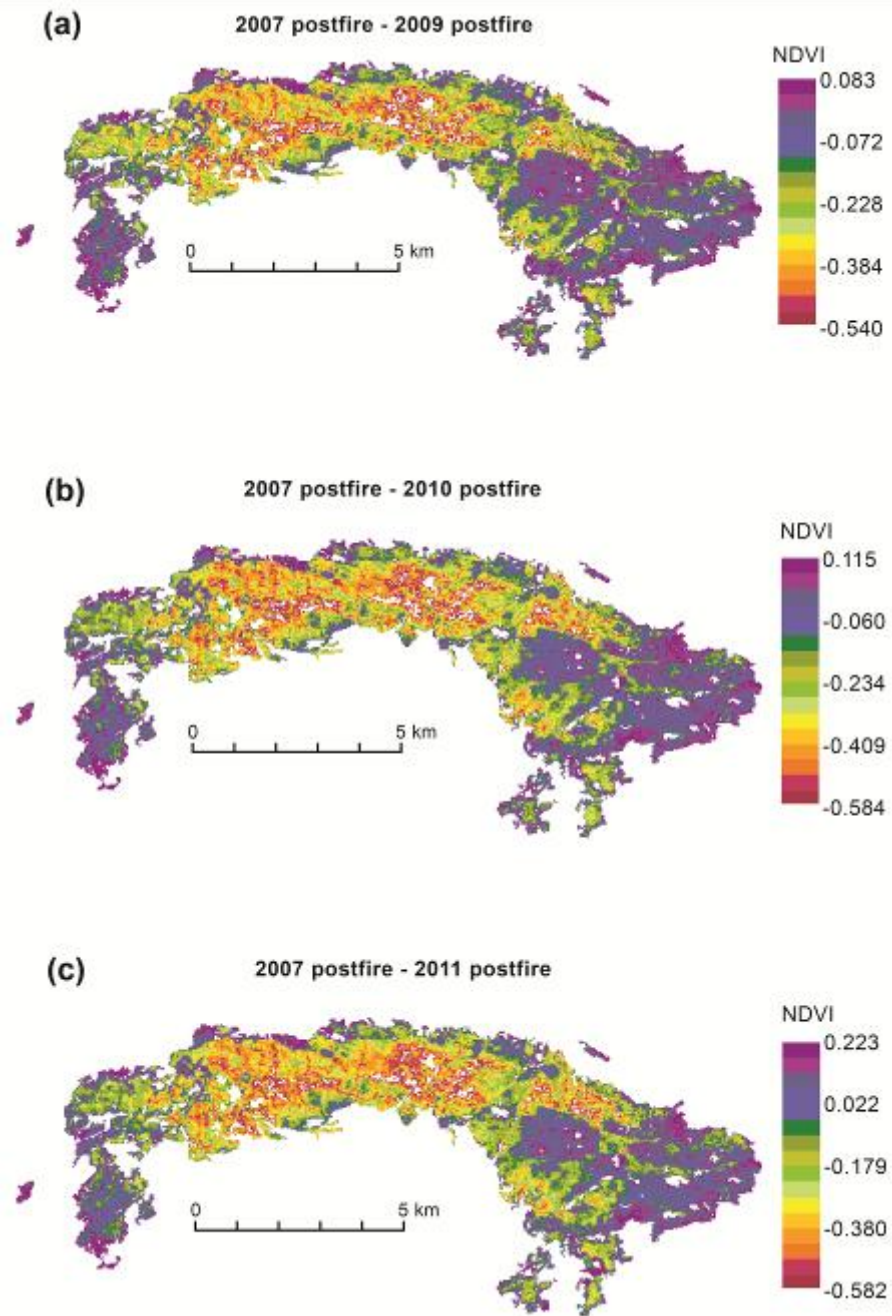


Figure 5: NDVI difference maps for the area under the burn scar, here between the post fire image in 2007 and all TM images after the fire suppression.

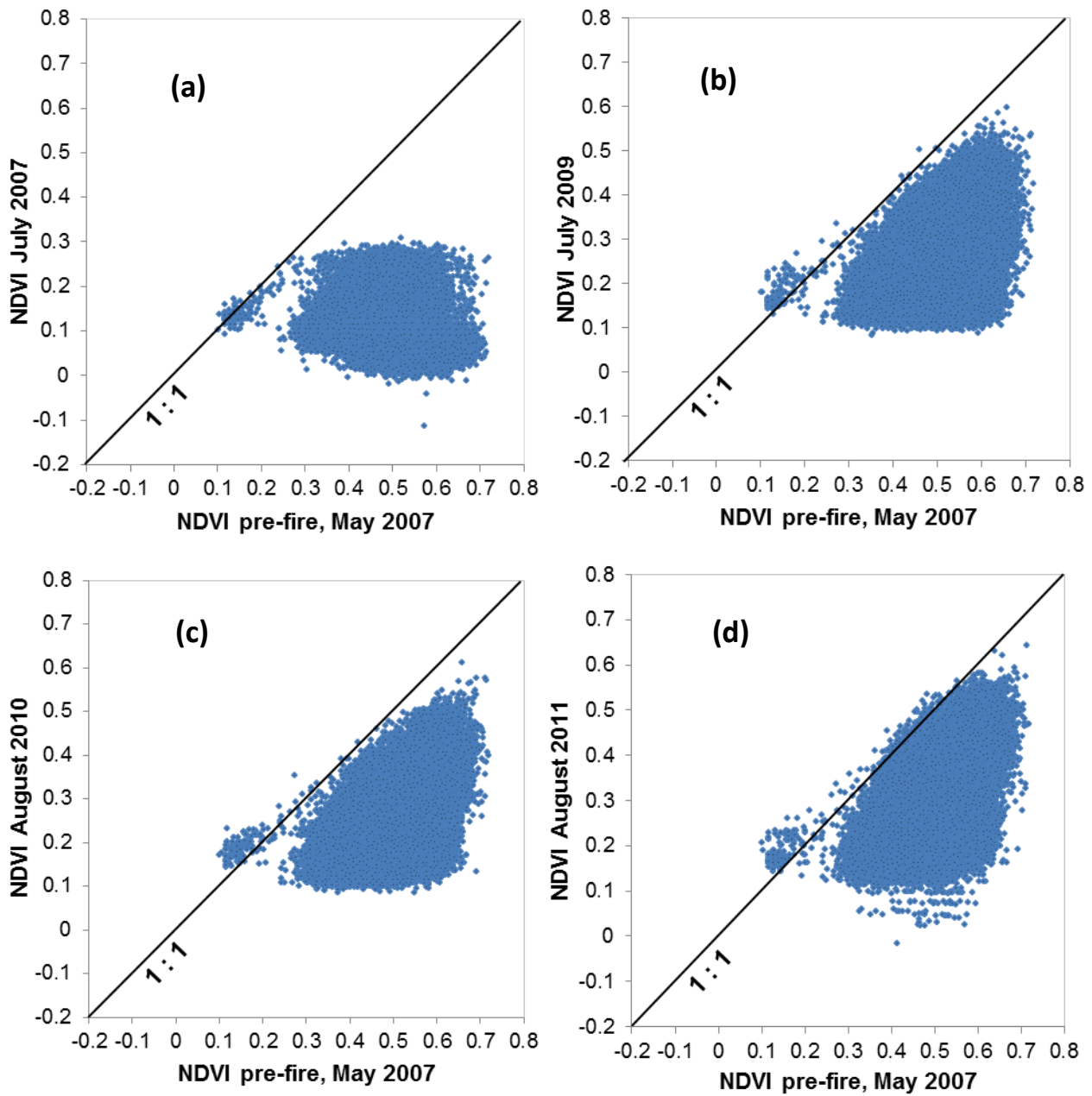


Figure 6: Scatterplots of pre-fire NDVI (May 2007) against (a) post-fire July 2007 (b) July 2009, (c) August 2010 and (d) August 2011. It can be observed the gradual increase of the slope to pre-fire conditions, which is suggesting re-growth in the area.

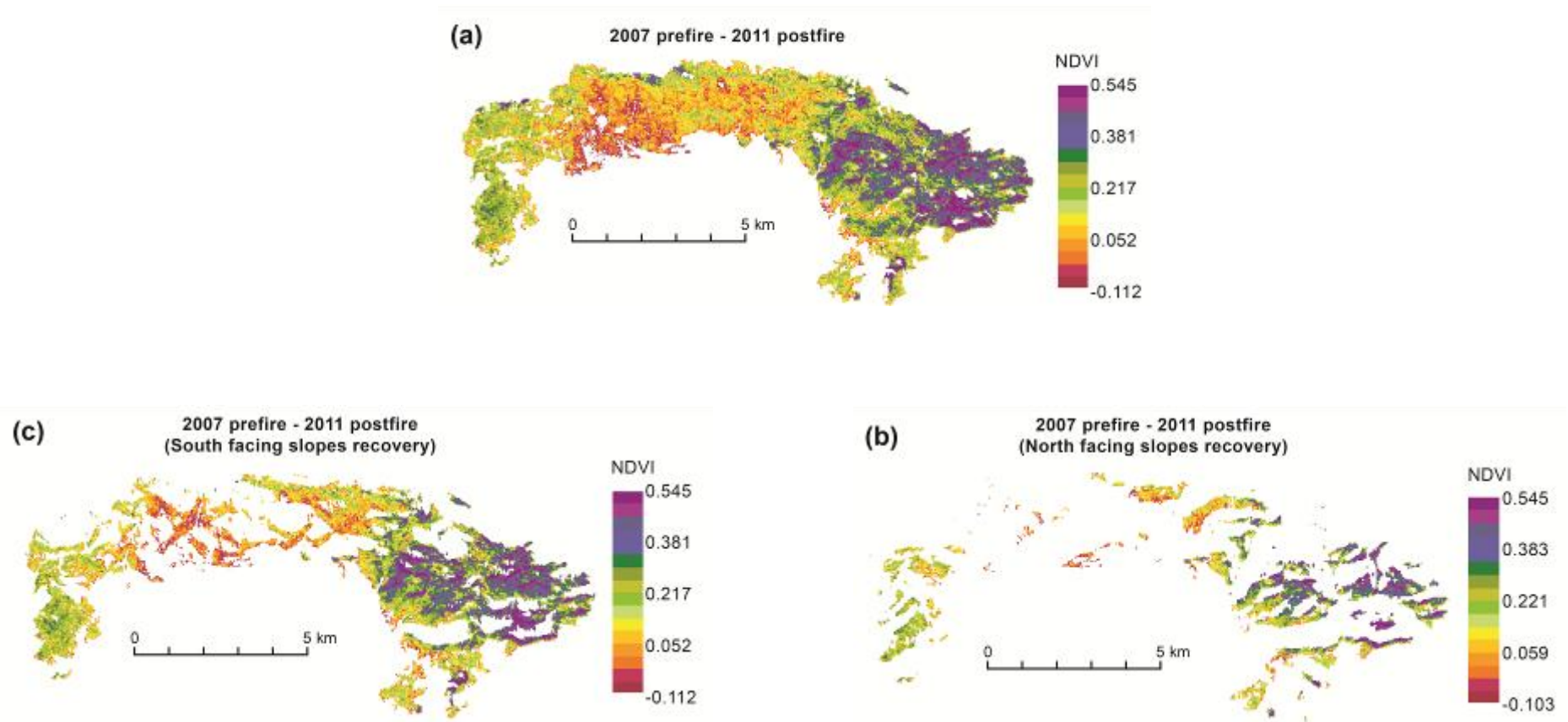


Figure 7: NDVI difference maps for the area under the burn scar, here between the pre-fire image and the most recent postfire image acquired in 2011 for a) the entire study area b) north facing slopes only and (c) south facing slopes only.

List of Tables:

Table 1: *NDVI changes for the area under the burn scar*

Landsat TM image date	NDVI			
	Min	Max	Mean	Stdev
16/05/2007	0.101	0.789	0.499	0.071
03/07/2007	-0.114	0.309	0.087	0.052
24/07/2009	0.083	0.597	0.259	0.092
12/08/2010	0.082	0.608	0.264	0.090
15/08/2011	-0.016	0.642	0.298	0.097

Table 2: *Scatterplot and correlation/regression analysis of the NDVI before and after the fire event for the whole area under the burn scar*

Period	Slope	Intercept	R ²
May 2007-July 2007	-0.215	0.194	0.086
May 2007-July 2009	0.495	0.012	0.148
May 2007 - August 2010	0.567	- 0.019	0.202
May 2007-August 2011	0.630	- 0.017	0.215

Table 3: NDVI changes for the area under the burn scar, separately for: (A): north facing, and, (B) south facing slopes.

NDVI				
(A). North facing slopes only				
Landsat TM image date	Min	Max	Mean	Stdev
16/05/2007	0.104	0.716	0.515	0.069
03/07/2007	-0.114	0.295	0.085	0.052
24/07/2009	0.099	0.597	0.300	0.090
12/08/2010	0.087	0.608	0.302	0.088
15/08/2011	0.095	0.622	0.340	0.094
(B). South facing slopes only				
Landsat TM image date	Min	Max	Mean	Stdev
16/05/2007	0.116	0.719	0.478	0.070
03/07/2007	-0.015	0.295	0.087	0.050
24/07/2009	0.083	0.526	0.218	0.077
12/08/2010	0.090	0.538	0.224	0.077
15/08/2011	0.026	0.582	0.253	0.083

Table 4: Scatterplot and correlation/regression analysis of the NDVI before and after the fire event separately for the north and south facing slopes only

Period	Slope	Intercept	R²
May 2007-July 2007			
North facing	-0.239	0.2090	0.103
South facing	-0.205	0.185	0.081
May 2007-July 2009			
North facing	0.537	0.023	0.103
South facing	0.356	0.048	
May 2007 - August 2010			
North facing	0.641	- 0.028	0.125
South facing	0.392	0.037	
May 2007-August 2011			
North facing	0.716	- 0.030	0.139
South facing	0.445	0.042	